Charge Localization in Collision-Induced Multiple Ionization of van der Waals Clusters with Highly Charged Ions

W. Tappe, R. Flesch, and E. Rühl

Fachbereich Physik, Universität Osnabrück, Barbarastrasse 7, 49069 Osnabrück, Germany

R. Hoekstra and T. Schlathölter

KVI Atomic Physics, Rijksuniversiteit Groningen, Zernikelaan 25, 9747AA Groningen, The Netherlands

(Received 13 November 2001; published 25 March 2002)

Charge localization in multiple ionization and fragmentation of small argon clusters is reported. The processes are initiated by interaction of the neutral cluster with highly charged Xe^{q+} ($5 \leq q \leq 25$). Products are detected by means of multicoincidence time-of-flight methods. A strong dependence of the fragmentation pattern on the Xe charge state q is observed. In particular, we find evidence for formation of multiply charged atomic Ar^{r+} fragment ions up to $r = 7$. Such high charge states have neither been observed in fission of multiply charged van der Waals clusters nor in ion-induced fragmentation of fullerenes or metal clusters. This hints at fundamentally different excitation and fragmentation dynamics.

DOI: 10.1103/PhysRevLett.88.143401 PACS numbers: 36.40.Qv, 34.70.+e, 36.40.Wa

Fragmentation and ionization dynamics of atomic and molecular van der Waals (VdW) clusters upon interaction with a variety of particles, for instance, electrons, photons, and metastable He atoms, have been investigated [1–4]. Multiply charged clusters can be efficiently prepared by core level excitation using soft x rays [4,5], multiple outer shell ionization by femtosecond laser radiation [5–8], or electron impact [1]. Mass spectrometry has provided critical sizes for stable doubly and multiply charged clusters [9]. Below the critical cluster size, which can accommodate the given number of charges, one observes the immediate decay of the multiply charged clusters. It is dominated by fission, where preferentially singly charged fragments are formed [4,5]. The fission mechanisms of doubly charged rare gas clusters have been investigated earlier by multicoincidence experiments [5] and molecular dynamics simulations [10]. These results indicate that fission of doubly charged clusters yields asymmetric pairs of singly charged products, which are formed along with a considerable kinetic energy. The amount of kinetic energy is often well described by a simple *Coulomb explosion* model [11].

The occurrence of multiply charged atomic fragments from VdW clusters has been observed only in experiments employing intense femtosecond lasers [6–8]. In this case the cluster is heated until it reaches the state of a hot plasma which subsequently undergoes fission. The amount of deposited energy is orders of magnitude larger than in other approaches. Atomic and molecular VdW clusters can reduce their internal energy by a variety of processes, such as emission of electrons and photons, evaporation of neutrals, or fission into fragments of various sizes. The relative importance of these channels depends primarily on the amount of energy that is deposited by initial excitation and ionization.

Highly charged ion (HCI) induced fragmentation and ionization of free clusters has been investigated only for strongly bound systems, such as fullerenes [12–15], and metal clusters [16–18]. Even though such interactions can lead to intermediate cluster charge states exceeding twice the HCI charge state, e.g., C_{60}^{60+} can be formed by Xe^{25+} impact, only singly and doubly charged atomic fragment ions were observed [19]. These results are rationalized by the high charge mobility in these cluster systems. The holes equilibrate on a femto- to picosecond time scale while fragmentation due to Coulomb explosion takes place on a somewhat slower time scale (cf. [10]). The interaction of multiply charged ions with VdW clusters offers, however, a different scenario. Here, the interatomic binding energies are considerably smaller and the electron mobility is lower, so that charge localization on single atomic sites can occur and multiply charged cations may be formed upon fission. This is the major motivation for this Letter in which we present the first experimental study of HCI interacting with VdW clusters. The HCI allows us to remove gently a large number of outer shell electrons within an ultrashort (femtosecond) time period, so that information on the ionization and fission mechanisms can be obtained.

The experiments have been performed using multiply charged ions extracted from the electron cyclotron resonance ion source located at the atomic physics facility of the Kernfysisch Versneller Instituut (Groningen, The Netherlands) [12]. We floated the source on a potential of 12 kV leading to Xe^{q+} velocities of $v = 0.14$, 0.21, 0.25, and 0.3 a.u. for $q = 5$, 12, 17, and 25, respectively.

The experimental setup was described earlier [4,20,21]. Briefly, argon clusters are produced by expanding the neat gas at a stagnation pressure $p_0 = 5$ bars through a 50 μm nozzle, which is kept at room temperature ($T_0 = 300$ K). The average cluster size $\langle N \rangle$ for these expansion conditions corresponds to $\sim$10 atoms (cf. [4,5]). The cluster jet is skimmed and transferred into a chamber where it is crossed with the collimated beam of highly charged Xe^{q+} ($5 \leq q \leq 25$) ions. Additional work was

performed using N^{q+} ($1 \leq q \leq 3$). The charged collision products are extracted by a moderate static electric field (300 V/cm) into a Wiley-McLaren-type time-of-flight (TOF) mass spectrometer of resolution $m/\Delta m \approx 125$. The mass spectrometer can be operated with either pulsed extraction voltages, where mass spectra are obtained, or static ion extraction, which is used for multicoincidence experiments, such as electron-ion-ion coincidences (cf. [5]). This also involves the detection of electrons. The electron detector is mounted opposite to the TOF. Multicoincidence spectra were recorded by using a multihit time-to-digital converter [22,23].

Figure 1 displays two TOF spectra as obtained from the collision of Xe^{5+} and Xe^{25+} with argon clusters at $\langle N \rangle = 10$. Both spectra are normalized to the Ar_2^+ peak intensity. Singly and multiply charged ions can be found at short flight times. Up to Ar^{8+} is found with mentionable intensity. Additional mass lines occur at longer flight times but with considerably lower intensity. These are due to Ar_n^+, reaching up to $n \gtrsim 10$ for both projectile charge states. For $q = 25$ the relative cluster yield is clearly smaller than at $q = 5$. Multiple cluster ionization is becoming more important, indicating that fragmentation via fission dominates. However, it is difficult to extract quantitative information from Fig. 1, since atomic argon, which dominates the cluster jet at $\langle N \rangle = 10$, can also yield multiply charged atoms. This problem is avoided by measuring time-correlated cations which originate exclusively from the decay of multiply charged clusters. Figure 2 shows a series of ion-ion coincidence spectra for various charge states of Xe^{q+} ($q = 5, 12, 17, 25$).

The ion-ion coincidence spectra show clear structures due to coincidences between singly and multiply charged atomic fragments. False coincidences are ruled out since these structures are not observed, if no clusters are present in the jet. The ion-ion coincidences are dominated by the Ar^+/Ar_2^+ channel for Xe^{5+} projectiles. But there is also some intensity that is due to Ar^+/Ar^{2+} coincidences. With projectiles of lower charge states (N^{q+}, with $1 \leq q \leq 3$) we observe only $Ar_{1,2}^+/Ar_n^+$ coincidences, with $n \leq 5$. This is similar to previous work on *K*- and *L*-shell excited argon clusters, where exclusively coincidences between singly charged cations were found [4,5,20–23]. This is mostly a result of low Ar charge states of $r \approx 2$ and $r \approx 4$ in the *L*- and the *K*-excitation regime, respectively.

With increasing charge state of Xe^{q+} two new series of ion-ion coincidences appear: Ar^+/Ar^{r+} and Ar^{2+}/Ar^{r+}. In both cases, we find for $q = 25$ that the fragment charge states range up to $r = 7$, i.e., Na-like argon. Such high fragment-ion charge states have not been observed before in HCI-induced cluster fragmentation. It is of particular interest that $r = 7$ is not observed in coincidence with fragment charge states higher than 2. This indicates a strongly localized primary ionization and only very limited

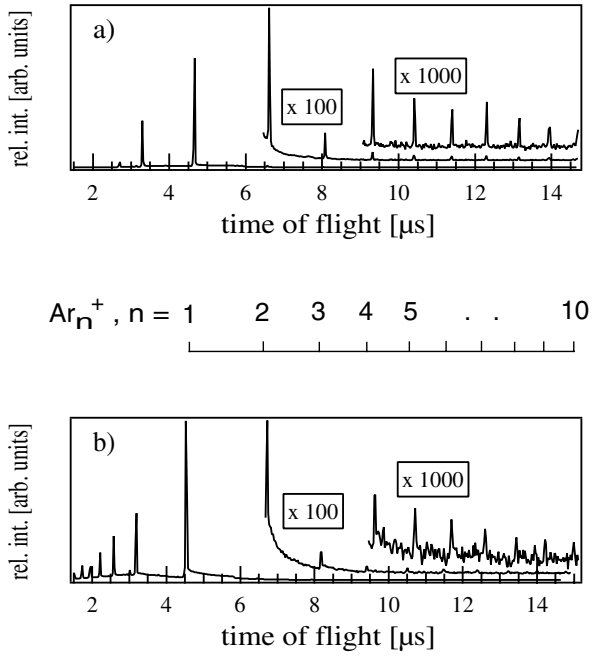

FIG. 1. Time-of-flight mass spectra of the collision products from Xe^{q+} collisions with argon clusters ($\langle N \rangle = 10$): (a) $q = 5$; (b) $q = 25$. Both spectra are normalized to the intensity of the Ar_2^+ mass line.

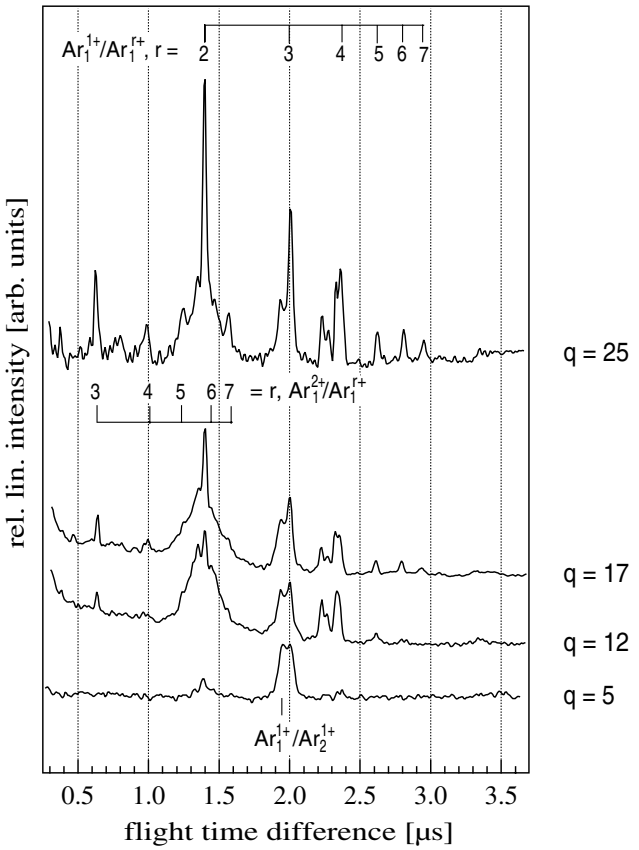

FIG. 2. Ion-Ion coincidence mass spectra of the products from Xe^{q+} collisions with Ar clusters ($q = 5, 12, 17, 25$).

charge equilibration before fission occurs. The coincidence mass spectra shown in Fig. 2 thus reflect a charge distribution far from an equilibrium.

From the classical overbarrier model (COB) [24] the critical distance R_r at which the projectile ion can capture the rth electron from the target can be estimated to be $R_r = [r + 2\sqrt{rq})]/I_r$ with the projectile charge state q and the rth ionization energy of argon I_r. This leads to values between $R_1 = 9.45$ a.u. ($q = 5$) and $R_1 = 19$ a.u. ($q = 25$). R_1 values that were obtained from experiments on absolute cross sections are only slightly smaller [25].

The maximum interaction length is thus $2 \times R_1$ for a central Xe^{q+}-Ar collision. In the case of a cluster target the cluster diameter ($\approx$ twice the Ar-Ar equilibrium distance of $D_{eq} \approx 3.78$ Å [20] for an Ar_{10} cluster) has to be added. With the projectile speed the maximum interaction time is estimated to be of the order of 4 fs (Xe^{5+}) and 6 fs (Xe^{25+}); more distant collisions proceed on an even shorter timescale. As a result, the collisions are completely nonadiabatic with respect to the motion of the atoms in a charged cluster which occurs on the picosecond time scale [10]. The cluster geometry can be expected to remain unchanged during the collision unless a direct Xe-Ar collision takes place, knocking an Ar atom out of the cluster.

With the COB we can also estimate the charge state distribution in the cluster, assuming an initially localized ionization of one of its constituent atoms. The COB neglects ion-ion interactions within the cluster, i.e., screening effects. Two different approaches are conceivable. In the "sequential" model the COB is applied first to the interaction of Xe^{q+} with the closest Ar atom (Ar') leading to an intermediate Ar'^{s+} after the collision. In the next step the COB is applied to the Ar'^{s+}-Ar systems; i.e., the interaction between the cluster constituents is treated. The intermediate Ar'^{s+} bound in a cluster participates in a charge transfer, where electrons from the outermost electronic shells of the surrounding atoms reduce the positive charge on the highly charged atom. This process is constricted by the initial Ar' charge as well as the capture distances between intermediate Ar'^{s+} and surrounding Ar atoms or ions. The highest observed charge of a correlated cation is $r = 7$. Thus, the last transfer of an electron to another site involves $Ar'^{(7+1)+}$. The first four capture radii for the Ar'^{8+} are estimated to be $R_{1,2,3,4} \approx 6.1$, 5.2, 4.5, and 3.7 Å. Only the last value falls below D_{eq}; i.e., formation of Ar'^{7+}-Ar^{4+} pairs is ruled out within this model. However, to observe Ar'^{7+}-Ar^{2+} pairs at least one nearest neighbor of Ar' has to be doubly ionized. Considering six nearest neighbors, the initial charge state of Ar'^{s+} had to be at least $Ar'^{(7+6+1)+}$. Even with a Xe^{25+} projectile, according to the COB the 14th electron is transferred only at a Xe-Ar' distance of less than 1 Å. At such close distances and high projectile q, all cluster constituents are affected by the Xe^{q+} presence. This fact is taken into account in the "simultaneous" scenario: Similar to the first case, Xe^{q+} removes electrons from the Ar' constituent. When Ar'^{3+} is formed, its potential in turn lowers the barrier to the surrounding Ar atoms sufficiently to allow electron transfer to Ar'^{3+}. Since the barrier between $Xe^{(q-3)+}$ and Ar'^{3+} is even lower, these electrons will be localized in the joint potential of $Xe^{(q-3)+}$ and Ar'^{3+}. For shorter X-Ar' distances Ar'^{4+} can be formed, allowing that another electron from the surrounding Ar^+ can participate in a charge transfer to the highly charged site. With Ar'^{5+} already triply charged surrounding ions are formed which in turn lower the potential barrier to their neighbors sufficiently to transfer their respective outermost electron. Stronger ionization starts only at Ar'^{9+}. Thus, with the highest observed charge state of a correlated ion ($r = 7$ for the Xe^{25+} case) only triply charged next neighbors and singly charged next-next neighbors can be formed. For $\langle N \rangle = 10$ this implies removal of up to 22 electrons from the cluster. For $Xe^{17+,25+}$, most probably all cluster constituents are ionized. For $q = 12$, r is reduced to 5, indicating incomplete cluster ionization. However, to obtain quantitatively correct results to compare to our experimental data, more accurate capture radii, for instance obtained from classical trajectory Monte Carlo calculations, are needed. First results indicate only small deviations from the COB model [26]. Our experimental data show only Ar^{7+}-Ar^{2+} coincidences but are statistically insufficient to rule out, e.g., Ar^{7+}-Ar^{3+} (see Fig. 2). Even though we expect the simultaneous model to describe the process best, more detailed studies are required.

Besides the fragment charge state r, the second fingerprint of the cluster deexcitation dynamics is the kinetic energy release (KER) due to the fragments mutual Coulomb repulsion. KER can be substantial, even in the case of VdW clusters with their large equilibrium distances [4,5,23]. For the charge separation distances in small argon clusters ($\langle N \rangle = 10$), we expect that Coulomb repulsion leads to KER $\approx$ 8–27 eV for Ar^+/Ar^{r+} ($r = 2$–7) and KER $\approx$ 23–53 eV for Ar^{2+}/Ar^{r+} ($r = 3$–7) coincidences. The TOF spectrometer transmission decreases strongly with kinetic energy of the detected particles that are emitted perpendicular to the spectrometer axis. In contrast, cations that have a substantial velocity component parallel to the spectrometer axis lead to double peak structures for KER $\gtrsim$ 5 eV as observed in previous coincidence work [4]. In the coincidence mode count rate is determined by the product of the different particle transmissions and depends strongly on the KER. For low KER events, as observed for Ar^{2+}/Ar^+ coincidences, even electron ion-ion coincidences can be measured without substantial mass discrimination (cf. Fig. 2). We acquired such triple coincidence data and their evaluation will be the subject of further studies.

The present results suggest an ionization and fragmentation mechanism to be active in VdW clusters undergoing collisions with highly charged ions, which is different from previous work on VdW clusters. The differences are

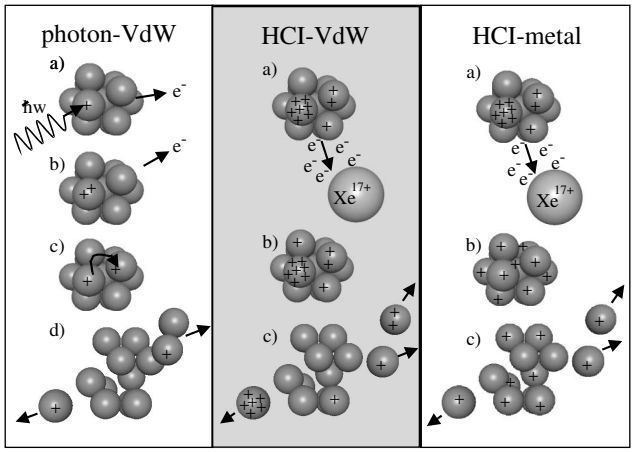

FIG. 3. Schematic mechanisms of ionization and fragmentation of small VdW clusters. Inner-shell excitation (left-hand panel) (a); photoionization with subsequent electronic relaxation (b); charge delocalization (c); fission (d). HCI collisions with VdW clusters (middle panel): collision (a); charge delocalization (b); fission (c). HCI collisions with metal clusters (right panel): collision (a); charge separation (b); fission (c).

visualized in Fig. 3. In the case of photoionization, a core electron of a cluster constituent is removed. A second electron is emitted from the same atom in an Auger deexcitation process. Subsequently, the charges separate and cluster fission occurs (cf. Fig. 3a). Ionization by a HCI removes several electrons on a short time scale. However, the cluster constituents behave as an ensemble of isolated atoms separated by the equilibrium distances in the cluster. Electrons are distributed over the cluster only within the limits of the COB model and fragment charge states up to $r = 7$ can remain localized (cf. Fig. 3b). This is fundamentally different to previous findings for HCI interaction with metal clusters and fullerenes [12–18]. Here, the electron removal step is similar to the VdW cluster case but, due to high charge mobility, complete charge equilibration takes place, thereby leading to the formation of at most doubly charged fragments (cf. Fig. 3c).

In conclusion, we found evidence for strong charge localization on VdW clusters which were ionized by means of HCI. To our knowledge, cluster fragment charge-state distributions far away from charge equilibration have not been observed before. This nonequilibrium arises from the particular conditions present in our experiment, i.e., fast and gentle electron removal from very weakly interacting cluster constituents. The charge distribution can be qualitatively explained within the framework of the classical overbarrier model.

R. H. and T. S. acknowledge financial support from the Stichting FOM supported by NWO and the LEIF network of the EU (HPRI-CI-1999-40012). T. S. is financially supported by the Royal Netherlands Academy of Arts and Sciences. Financial support by the Fonds der Chemischen Industrie and Deutsche Forschungsgemeinschaft are gratefully acknowledged.

[1] (a) *Clusters of Atoms and Molecules,* edited by H. Haberland (Springer, Berlin, 1994), Vol. I; (b) *Clusters of Atoms and Molecules,* edited by H. Haberland (Springer, Berlin, 1995), Vol. II.
[2] P. Scheier and T. D. Märk, J. Chem. Phys. **86**, 3056 (1987).
[3] H. Tanaka, R. Maruyama, Y. Yamakita, H. Yamakado, F. Misaizu, and K. Ohno, J. Chem. Phys. **112**, 7062 (2000).
[4] E. Rühl, H. W. Jochims, C. Schmale, E. Biller, M. Simon, and H. Baumgärtel, J. Chem. Phys. **91**, 6544 (1991).
[5] E. Rühl, C. Heinzel, H. Baumgärtel, M. Lavollée, and P. Morin, Z. Phys. D **31**, 245 (1994).
[6] E. M. Snyder, S. A. Buzza, and A. W. Castleman, Jr., Phys. Rev. Lett. **77**, 3347 (1996).
[7] T. Ditmire, J. W. G. Tisch, E. Springate, M. B. Mason, N. Hay, J. P. Marangos, and M. H. R. Hutchinson, Phys. Rev. Lett. **78**, 2732 (1997).
[8] M. Lezius, S. Dobosz, D. Normand, and M. Schmidt, Phys. Rev. Lett. **80**, 261 (1998).
[9] O. Echt and T. D. Märk, in Ref. [1(b)], p. 183.
[10] J. G. Gay and B. J. Berne, Phys. Rev. Lett. **49**, 194 (1982).
[11] T. A. Carlson and M. O. Krause, Phys. Rev. **137**, 1655 (1965).
[12] T. Schlathölter, R. Hoekstra, and R. Morgenstern, J. Phys. B **31**, 1321 (1998).
[13] S. Martin, L. Chen, A. Denis, and J. Desesquelles, Phys. Rev. A **57**, 4518 (1998).
[14] J. Opitz, H. Lebius, B. Saint, S. Jacquet, B. A. Huber, and H. Cederquist, Phys. Rev. A **59**, 3562 (1999).
[15] B. Walch, C. Cocke, R. Voelpel, and E. Salzborn, Phys. Rev. Lett. **72**, 1439 (1994).
[16] F. Chandezon, C. Guet, B. A. Huber, D. Jalabert, M. Maurel, E. Monnand, C. Ristori, and J. C. Rocco, Phys. Rev. Lett. **74**, 3784 (1995).
[17] C. Guet, X. Biquard, P. Blaise, S. A. Blundell, M. Gross, B. A. Huber, D. Jalabert, and M. Maurel, Z. Phys. D **40**, 317 (1997).
[18] L. Plagne and C. Guet, Phys. Rev. A **59**, 4461 (1999).
[19] S. Martin, L. Chen, A. Denis, and J. Desesquelles, Phys. Rev. A **59**, R1734 (1999).
[20] E. Rühl, C. Heinzel, A. P. Hitchcock, and H. Baumgärtel, J. Chem. Phys. **98**, 2653 (1993).
[21] E. Rühl, C. Heinzel, A. P. Hitchcock, H. Baumgärtel, H. Schmelz, C. Reynaud, W. Drube, and R. Frahm, J. Chem. Phys. **98**, 6820 (1993).
[22] E. Rühl, A. P. Hitchcock, P. Morin, and M. Lavollée, J. Chim. Phys. Phys.-Chim. Biol. (France) **95**, 521 (1995).
[23] E. Rühl, A. Knop, A. P. Hitchcock, P. A. Dowben, and D. N. McIlroy, Surf. Rev. Lett. **3**, 557 (1996).
[24] A. Bárány, J. Phys. B **19**, 2925 (1986).
[25] N. Selberg, C. Biedermann, and H. Cederquist, Phys. Rev. A **54**, 4127 (1996).
[26] R. E. Olson (private communication).